Research Article

Journal of RAMAN SPECTROSCOPY

Received: 2 April 2008 Accepted: 5 July 2008 Published online in Wiley Interscience: 24 September 2008

(www.interscience.wiley.com) DOI 10.1002/jrs.2084

Surface-enhanced Raman scattering spectroscopy via gold nanostars

E. Nalbant Esenturk and A. R. Hight Walker*

Anisotropic metallic nanoparticles (NPs) have unique optical properties, which lend them to applications such as surface-enhanced Raman scattering (SERS) spectroscopy. Star-shaped gold (Au) NPs were prepared in aqueous solutions by the seed-mediated growth method and tested for Raman enhancement using 2-mercaptopyridine (2-MPy) and crystal violet (CV) probing molecules. For both molecules, the SERS activity of the nanostars was notably stronger than that of the spherical Au NPs of similar size. The Raman enhancement factors (EFs) for 2-MPy on Au nanostars and nanorods are comparable and estimated as greater than 5 orders of magnitude. However, the enhancement for CV on nanostars was significantly higher than for nanorods, in particular at CV concentrations of 100 nM or lower. This article is a US Government work and is in the public domain in the USA. Published in 2008 by John Wiley & Sons, Ltd.

Supporting information may be found in the online version of this article.

Keywords: gold nanoparticles; nanostar; crystal violet; 2-mercaptopyridine; SERS

Introduction

Surface-enhanced Raman scattering (SERS) spectroscopy has received a great deal of attention for its utility as a sensitive technique for chemical and bioanalytical sensing and imaging.[1–4] Noble metal nanoparticles (NPs) (Ag and Au) are the most commonly used SERS substrates both in colloidal solutions and on solid surfaces.[1–13] They have advantages such as ease of formation and handling, and tunable size- and shape-dependent optical properties. In particular, the noble metal NPs with nonspherical morphologies have directed researchers to examine these particles' Raman enhancing capabilities due to their distinctive optical properties.[6–14]

Chemical and electromagnetic enhancements are two effects commonly considered as the origin of the enhanced Raman signal.[15,16] The former depends on the nature of the molecule and results from an increased molecular polarizability by formation of a charge-transfer complex between the metal surface and the molecule.[16] This generally results in disparate enhancement factors (EFs) for different molecules on identical SERS substrates. Molecules with delocalized electrons such as lone pairs or π clouds (e.g. aromatic amines, phenols) often demonstrate strong Raman enhancement. The electromagnetic component of the enhancement results from an increased field at the metallic NP surface. The field enhancement is a consequence of the interaction of the incoming laser radiation with electrons in the metal surface, which activates surface plasmons, or collective oscillations of the metal electrons.[15] It has been observed that aggregates of metallic NPs generate very intense enhanced Raman signals at the junction between two NPs, called 'hot spots'.[3,17] Similar increased fields are also found at the tips of NPs with sharp features, such as rods or triangles.[6,7,14,18–20] Therefore, anisotropic, metallic NPs are great candidates for SERS substrates and an active area of research.

Here, we present a SERS study of star-shaped Au NPs in aqueous solution using 2-mercaptopyridine (2-MPy) and crystal violet (CV) molecules to evaluate their Raman enhancing properties. The SERS activity of the star-shaped NPs is compared with that of Au nanospheres and nanorods of complementary sizes.

Experimental

$HAuCl_4^{\cdot}H_2O$, $NaBH_4$, ascorbic acid, $AgNO_3$, and cetyltrimethylammonium bromide (CTAB) were purchased from Aldrich (Certain commercial equipment, instruments, or materials are identified in this paper to adequately specify the experimental procedure. In no case does identification imply recommendation or endorsement by NIST.) and used without further purification. Gold colloids (e.g. 10 and 150 nm spherical) were purchased from Ted Pella. Ultrapure deionized water (resistivity greater than 18.0 MΩ cm) was used for all solution preparations and experiments.

Star-shaped Au NPs were prepared in aqueous phase via the surfactant-directed, seed-mediated growth method as described in the literature.[19] Growth solution was prepared by adding 0.200 ml of 0.01 M $HAuCl_4^{\cdot}H_2O$ to 4.5 ml of 0.1 M CTAB in a plastic test tube while gently mixing. To this solution, 0.030 ml 0.01 M $AgNO_3$ was added. After mixing, the color of the solution becomes brownish yellow. Then, 0.032 ml of 0.1 M ascorbic acid was added, resulting in a colorless solution. Finally, 0.01 ml of 10-nm commercially available seed solution was added. After gentle mixing, the solution was kept in a water bath at room temperature undisturbed for 3 h. The eventual blue-purple color of the growth solution indicates nanostar formation. Energy-dispersive X-ray ((EDX) study showed the composition of nanostars as *ca* 96% Au, *ca* 2% Ag and *ca* 2% Br (see Supporting Information

* *Correspondence to: A. R. Hight Walker, Optical Technology Division, Physics Laboratory, National Institute of Standards and Technology, Gaithersburg, MD 20899-8443, USA. E-mail: angela.hightwalker@nist.gov*

Optical Technology Division, Physics Laboratory, National Institute of Standards and Technology, Gaithersburg, MD 20899-8443, USA

This article is a US Government work and is in the public domain in the USA. Published in 2008 by John Wiley & Sons, Ltd.

Journal of RAMAN SPECTROSCOPY

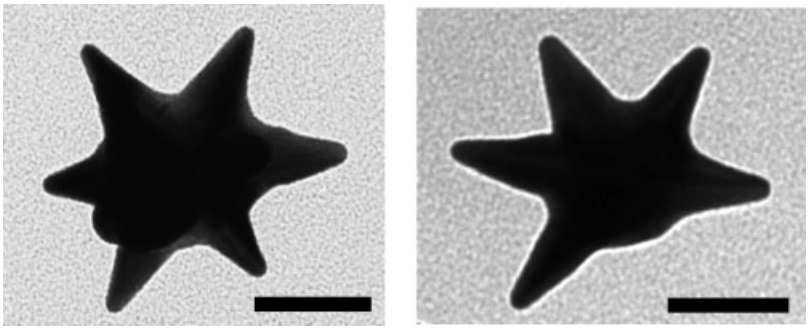

Figure 1. TEM images of star-shaped gold nanoparticles. The scale bars are 50 nm.

for EDX data). Transmission electron microscopy (TEM) images verified star-shaped nanostructures with an average size of *ca* 140 nm (Fig. 1). These NPs have three-dimensional structures with various numbers of tips growing out of the NP core. Analysis of over 100 NPs via TEM revealed that more than 90% of them have at least one tip or more (see Supporting Information for additional images and size and number of tips distribution). Since TEM is a two-dimensional analysis method, the tips in the third dimension may not be observed, thus this analysis shows only a minimum number of tips of these nanostructures. The UV–vis absorption measurements of the colloidal nanostar solution demonstrated plasmon bands around 600 and 900 nm, the breadth of which is most likely due to the structural diversity (Fig. 3 inset).

Nanorods with an aspect ratio of *ca* 2 were also prepared using the seed-mediated growth method.[21] First, a seed solution of Au was prepared by adding 0.25 ml of 0.01 M $HAuCl_4^{-}H_2O$ with 7.5 ml of 0.1 M CTAB and gently mixing. While stirring, ice-cold 0.6 ml of 0.01 M $NaBH_4$ was added to the solution, and mixed for an additional *ca* 2 min as the evolved gas was allowed to escape. The solution was kept at room temperature and used within 3 h of preparation. Finally, 2 µl of the prepared seed solution, containing $HAuCl_4.H_2O$, CTAB, $AgNO_3$ and ascorbic acid, was added to the growth solution as described in the previous paragraph. Similar to nanostars, nanorods are also composed of *ca* 96% Au, *ca* 2% Ag and *ca* 2% Br (see Supporting Information for EDX data).

The TEM images of NPs were acquired using a Zeiss EM 10 CA instrument at an acceleration voltage of 80 kV. Also, a Shimadzu model UV-1601 dual beam UV–vis spectrometer with scan range of 300–1100 nm was used to observe formation and/or aggregation of NPs. EDX measurements were performed on JEM 2100 FEG.[20] Raman measurements were made with a Renishaw RM 1000 Raman microscope equipped with 632.8 nm He–Ne excitation laser. The sampling technique involved placing a 1-cm path length cuvette at focus of a 5× microscope objective mounted on an L-shaped adapter. Samples were illuminated with *ca* 3 mW of power. Spectral data was collected in the continuous scan mode over the range 300–1700 cm^{-1} with 120 s integration time. A slit width of 20 µm was used before a 1800 grooves/mm holographic grating coupled to a RenCam charge-coupled device (CCD) detector.

SERS samples were prepared by mixing 1 ml of Au colloid solution with 0.1 ml of aqueous probe molecule (2-MPy or CV) solution at varying concentrations. The samples were sonicated *ca* 10 min prior to the measurements. For samples in which NaCl was used to induce the aggregation, 1 ml of NaCl solution was added to 1 ml of Au NP solution. After *ca* 10 min of sonication, 0.1 ml probe molecule solution was added, and the final mixture was sonicated for *ca* 10 min before acquiring the SERS spectra.

Results and Discussion

The enhanced Raman signal strength of colloidal Au NPs is dependant upon multiple factors including NP concentration, shape, and aggregation state, as well as the analyte (probe molecule) type and its concentration in the sample solution. Throughout our comparison of SERS activity, optimum NP concentrations were chosen such that strongest SERS signal intensity could be achieved for each type of NP. The results are presented in the following sections.

2-Mercaptopyridine

Raw Raman and SERS spectra of 2-MPy are presented in Fig. 2. The number of vibrational modes detected and their relative intensities were reproducible for day-to-day and batch-to-batch measurements of nanostar solutions. The peak assignments of bulk and adsorbed 2-MPy on Au NPs are based on those previously reported.[5] The vibrational modes observed in the SERS spectra (Fig. 2(a)) are in good agreement with those reported for 2-MPy on Ag electrodes and Ag NPs.[5,22] The red shift in the modes involving ν(C–S) at 731 cm^{-1} to 717 cm^{-1} and of ring breathing (RB)/ν(C–S) band at 1141 to 1117 cm^{-1} demonstrates chemisorptions of 2-MPy to the Au surface through the sulfur atom. The relatively

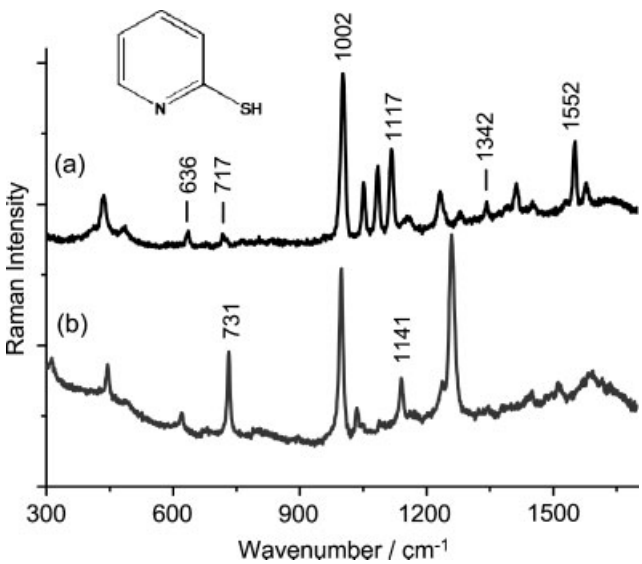

Figure 2. (a) SERS spectra of 1 µM 2-MPy on Au nanostars and (b) Raman spectra of 0.1 M 2-MPy. Inset shows chemical structure of 2-MPy molecule. Traces are offset for clarity.

This article is a US Government work and is in the public domain in the USA. Published in 2008 by John Wiley & Sons, Ltd.

weak enhancement of the C–S stretching mode at 717 cm^{-1} suggests that the C–S bond is not fully perpendicular to the metal surface.[5] Strongly enhanced in-plane stretching and RB modes such as ν(C=C) at 1552 cm^{-1}, ν(C–H) at 1085 cm^{-1}, RB at 1002 cm^{-1}, and RB/ν(C–S) at 1117 cm^{-1} imply perpendicular arrangement for the plane of the molecule to the metal surface. On the other hand, the presence of out-of-plane vibration modes such as γ(CCC) at 636 cm^{-1} and γ(CH) at 1342 cm^{-1} and the strongly enhanced out-of-plane bending mode β(CH) at 1051 cm^{-1} suggests more parallel orientation with respect to the surface. The multiple strong enhancements observed for both in-plane and out-of-plane modes suggest either (1) molecules oriented both perpendicular and parallel or (2) molecular adsorption to the surface with a broad angular distribution. Both are likely due to the complex three-dimensional nature of the nanostars surface.

Aggregated NPs are known to be the effective systems for SERS studies as they provide multiple particle junctions, and thus more 'hot spots'.[3,23] The addition of salt (e.g. NaCl) to a solution of NPs, 'salt-induced aggregation', is a common method to achieve aggregation of NPs and provide more 'hot spots'.[3,13,24] The aggregation process is generally explained by electrostatic interaction of the Cl^- ion with the surfactant-coated NP surface. This causes a decrease in repulsion between NPs and leads to coagulation.[25,26] Similar to the reported studies of other NP systems,[13,27,28] we observe a dependence of NaCl concentration in the measured SERS signal strength. Although most of the major vibrational modes of 2-MPy adsorbed on nanostars were detectable without addition of NaCl, an increase in the enhanced Raman signal was observed at an optimum concentration of NaCl (*ca* 50 mM in SERS sample). The aggregation process was evident by a change in the colloidal solution color (turning pale) with the addition of NaCl. Moreover, the UV–vis spectra of the aggregated Au nanostars solution showed a decrease in plasmon intensity (Fig. 3 inset).

The concentration of the analyte, 2-MPy, also plays a crucial role in the SERS activity of gold nanostars (Fig. 4). Enhanced Raman signal strength was weakest at low 2-MPy concentrations

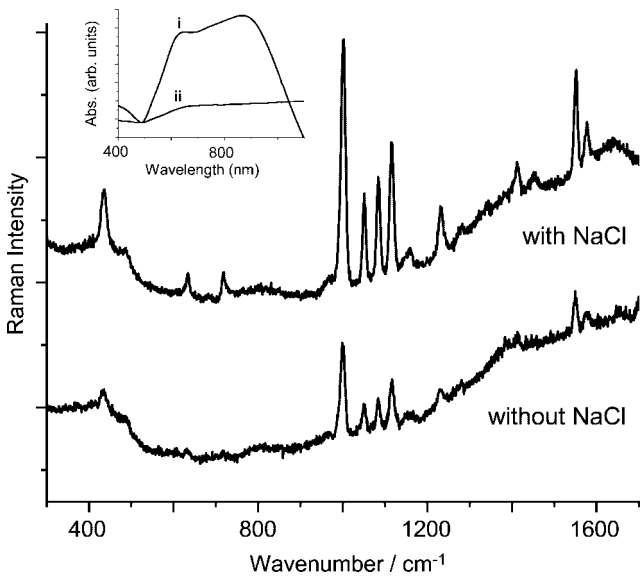

Figure 3. SERS activity of Au nanostars as a function of NaCl addition. Inset shows UV–vis spectra of (i) before NaCl addition (only nanostar solution) and (ii) after NaCl addition (50 mM to SERS sample). 2-MPy concentration was kept constant at 1 μM in SERS sample. Traces are offset for clarity.

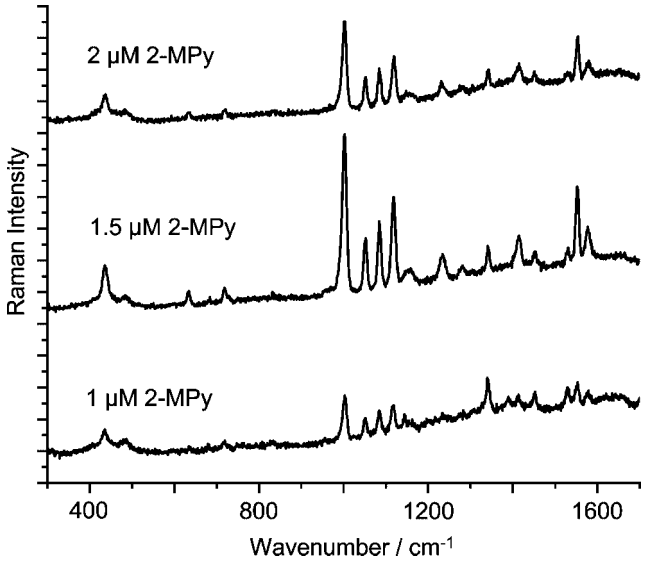

Figure 4. SERS activity of Au nanostars as a function of 2-MPy concentration. 2-MPy concentrations in SERS sample are shown on the figure. NaCl concentration was kept constant at 50 mM. Traces are offset for clarity.

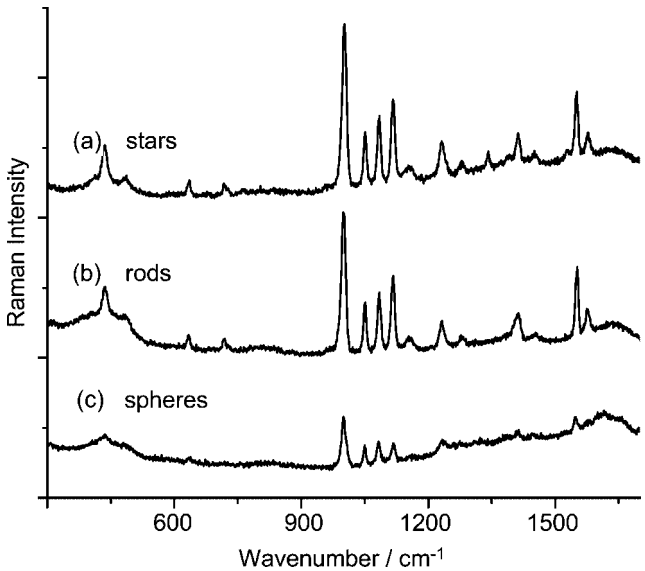

Figure 5. SERS spectra comparison of 2-MPy adsorbed on Au (a) nanostars (*ca* 140 nm), (b) nanorods (*ca* 65 nm × 30 nm (length × width)), and (c) nanospheres (*ca* 150 nm). Traces are offset for clarity.

(e.g. 0.5 μM). It increased as the 2-MPy concentration increased and reached a maximum at 1.5 μM. Further addition of the analyte decreased the SERS signal. A proposed explanation for the observed dependence of the intensity on analyte concentration is as follows. There were not enough molecules to cover the surface of the NPs at the lowest concentration.[4] Saturation likely occurred close to a molecular concentration of 1.5 μM owing to full coverage of the NP surface by 2-MPy. Above the saturation point, the excess molecules form additional layers, resulting in lower electromagnetic and chemical contribution to the enhancement and thus a decrease in the observed SERS signal intensity.[12]

We also studied the SERS activity of aggregated Au nanospheres and nanorods of complementary sizes to compare against the enhancing properties of the nanostars (Fig. 5). Au spheres between

This article is a US Government work and is in the public domain in the USA. Published in 2008 by John Wiley & Sons, Ltd.

the sizes of 50 to 200 nm produced similar SERS signals to one another when all other parameters were kept equal. The observed Raman enhancement by all the sizes of the nanospheres was less than that of the nanostars and is described further in the following paragraphs. To compare the SERS activities of Au nanorods to nanostars, nanorod sizes were selected that produce plasmon bands close to our excitation source (632.8 nm) to obtain the maximum possible electromagnetic contribution to the enhancement. Approximately 65 nm long by 30 nm wide nanorods with absorption bands at 700 and 550 nm were used. These nanorods produce SERS activity similar to that of the nanostars. However, two modes, at 1341 cm^{-1} (γ (CH)) and 1530 cm^{-1} (ν(C═C/C═N)), are unique to nanostars samples, and the mode at 1450 cm^{-1} (ν(C═C/C═N)) was more strongly enhanced with samples containing nanostars compared to nanorods. These modes were tentatively assigned to 2-MPy, but since the wavenumbers are in close proximity with those of the surfactant molecule CTAB,[8] they were not used to estimate an EF.

EF calculations for aggregated systems are difficult because of the fact that the number of molecules adsorbed either on 'hot spots' or on the rest of the NP surface is not known.[8] It is even more difficult to perform this calculation for star-shaped NPs because of their nonuniform, three-dimensional structures. Therefore, we have estimated a rough *lower limit* EF for certain modes by comparing the signal intensities in the measured SERS spectrum of 2-MPy on nanostars to the bulk Raman spectrum of the molecule. The following expression[13,29] was used to estimate the EF:

$$EF = [I_{SERS}]/[I_{Raman}] \times [M_{bulk}]/[M_{ads.}] \quad (1)$$

where I_{SERS} and I_{Raman} are intensities of a vibrational mode in SERS and Raman spectra, respectively. M_{bulk} is the concentration of the molecules in the bulk sample used in the Raman measurement, and M_{ads} is the concentration of the adsorbed molecules on the Au surface. 2-MPy concentrations of 0.1 M and 1×10^{-6} M were used for the Raman and SERS measurements, respectively. The assumption was made that all the 2-MPy in the SERS sample solution were adsorbed on the Au NPs. The I_{SERS} and I_{Raman} were measured for the RB mode at 1002 cm^{-1}. The *lower limit* of the EF for the aggregated nanostars is calculated as ~5 orders of magnitude but is likely much higher for nanostars as we assumed adsorption of all the 2-MPy molecules in the solution on the NPs surface, and equal contribution to the measured intensity of the modes from each molecule. The same EF calculation for nanospheres, discussed below, revealed an order of magnitude lower EF for the same vibrational mode.

The relatively uniform surface of nanospheres (compared to nanostars) permits a surface area calculation and thus enables use of estimated 2-MPy concentration in the EF estimation. The 150-nm diameter spheres with a plasmon band near 600 nm were chosen for this calculation owing to their similar size to the nanostars. The maximum number of 2-MPy molecules adsorbed on the nanosphere surface was estimated by using the nanosphere surface area and reported surface coverage area of 2-MPy (0.18 nm^2).[30,31] The concentration of 2-MPy molecules to cover the surface area of 150 nm Au nanospheres (at a concentration of 7×10^{-13} M) was calculated to be 5×10^{-7} M. Experimentally however, larger amounts were necessary to observe saturation, likely due to adsorption efficiency. Using the calculated concentration of 2-MPy (5×10^{-7} M), the EF is estimated as *ca* 5×10^4 for nanospheres for the RB mode. It is difficult to estimate accurately the concentration and surface area of nanostars because of their nonuniform three-dimensional structures. Therefore, EFs for nanostars were estimated by comparing the SERS intensity of the modes with those of nanospheres since the optimum NP concentration was used for both types of NPs. The Au nanostars show approximately 4 times more enhancement in the SERS spectrum for the RB mode and even higher enhancements for most of the other modes suggesting an EF for nanostars of greater than *ca* 2×10^5. The estimated EF value is similar to that calculated in the previous paragraph where the actual concentration of 2-MPy added to the solution was used.

EF for nanorods estimated in similar ways is approximately equivalent to that estimated for nanostars at 5 orders of magnitude. EF comparisons of nanostars with nanorods and nanospheres may contain considerable error because of the use of different surfactants (CTAB *versus* citrate) to stabilize the NPs, which may produce differences in surface chemistries, and also possible difference in NP concentrations in solutions.

Crystal violet

Our SERS investigation of Au nanostars with CV also revealed strong enhancement of the vibrational modes. As in the 2-MPy study, all vibrational modes with similar relative intensities were observed for all the batches of nanostar solutions. The SERS and bulk Raman spectra of CV are shown in Fig. 6. The spectral assignments were based on the study by Persaud and Grossman.[32] The vibrational modes of CV observed in our SERS spectra also agree well with those of Cialla *et al*.[20] on array-like gold nanostar and nanodiamond structures prepared using electron lithography. Three different groups of modes were observable for CV: modes associated with (1) the central carbon atom (C^+ – phenyl vibrations, up to 450 cm^{-1}), (2) nitrogen atoms (N–phenyl stretching, between 1350 and 1400 cm^{-1}), and (3) phenyl rings (skeletal ring vibrations and ring C–H deformations between 400 and 1300 cm^{-1}, and ring stretching modes above 1400 cm^{-1}). While all these modes were strongly

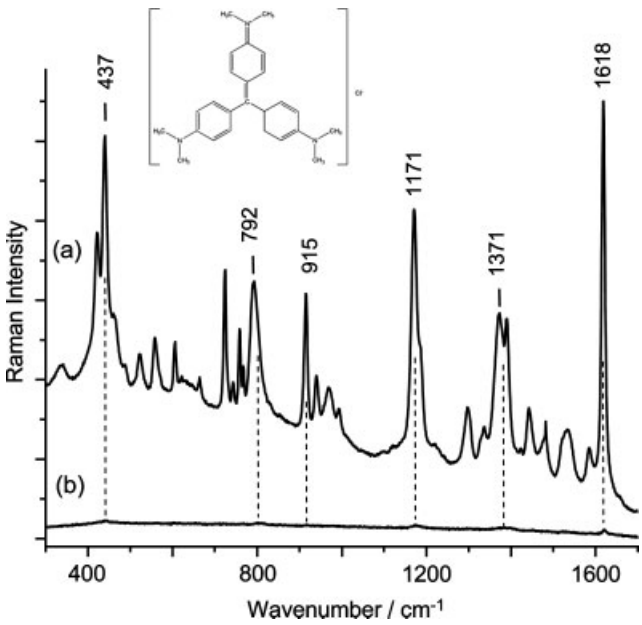

Figure 6. (a) SERS spectra of 0.1 μM CV on Au nanostars and (b) Raman spectra of 1 mM CV. Traces are offset for clarity. Vertical lines mark positions of some characteristic vibrational bands of CV.

This article is a US Government work and is in the public domain in the USA. Published in 2008 by John Wiley & Sons, Ltd.

enhanced on Au nanostars in our SERS measurements, only a few were detectable in the bulk Raman spectra of CV. The features used for enhancement comparison were the C^+ – phenyl bending at 336 cm^{-1}, ring C–H bending at 792 and 1171 cm^{-1}, ring skeletal vibration of radical orientation at 915 cm^{-1}, N–phenyl stretching at 1371 and 1391 cm^{-1}, and ring C–C stretching at 1531 and 1618 cm^{-1}. A comparison of SERS and Raman spectra of the molecule shows only small shifts of these modes, making it difficult to determine the adsorption site of the molecule on the Au NP surface. The results suggest that CV and Au NPs do not interact strongly. On the other hand, the strong enhancements observed for all groups of modes mentioned previously suggest the central carbon atom, nitrogen atoms, and π electrons in the phenyl ring as possible interaction sites.[32]

The effect of salt-induced aggregation and analyte concentration on the enhanced Raman signal intensity of CV vibrational modes was also investigated. The addition of NaCl did not provide significant improvement of the observed signal intensity. This is most likely due to the ionic character of CV. Similar to our 2-MPy study, an increase, saturation, and decrease in the signal intensity was noted upon changing of CV concentration in the nanostar solution. The optimum CV concentration is *ca* 1.6 μM (Fig. 7(c)).

As in our 2-MPy study, we compared the SERS activity of Au nanostars with that of nanospheres and nanorods using CV as the probe molecule (Fig. 7). Again, complementary sizes of nanospheres and nanorods were used. For CV, the SERS activities of the NPs were compared at various concentrations of the molecule due to differences in optimum CV concentration for each shape of NPs. Au nanostars showed the highest Raman enhancement at all concentrations studied, between 0.1 and 1.6 μM, compared to the enhancement observed either with nanorods or with nanospheres. With nanostars, most of the CV modes were detectable even at lower CV concentrations such as at 1 nM. On the other hand, the modes were barely or not at all detectable at 100 nM of CV concentration in the nanosphere or nanorod solutions. The CV concentration needed to be increased by approximately a factor of 10 (i.e. to 0.8 μM) to reach optimum concentration where the strongest SERS intensity was achieved for nanorods (Fig. 7(b)). No significant intensity change was observed with nanospheres at the concentration range studied (Fig. 7). The stronger enhancement for nanostars compared with nanorods and nanospheres is likely due to the obvious structural differences of the NPs. Nanostars are expected to have more SERS-active sites ('hot spots') because of their anisotropic shapes compared to nanorods and nanospheres. Furthermore, the molecules may preferentially adsorb on these sites, making detection at notably lower adsorbate concentrations possible. Kudelski[33] reported preferential adsorption of the CV molecules at highly SERS-active sites on electrochemically roughened silver surfaces. Our observed differences in the relative activity of these distinct NPs shapes at low CV concentrations also suggest the preference of CV molecules toward highly SERS-active sites.

The EF for specific modes of CV was estimated following the methods described in the 2-MPy section of this paper. Signal intensities of the ring C–C stretching mode at 1618 cm^{-1} in the measured SERS and bulk Raman spectra of the molecule (1 mM) were used to calculate the EF at three different concentrations of CV (0.1, 0.8, and 1.6 μM) in NP solutions. The EF for nanostars was estimated as *ca* 5×10^5 at 0.1 μM CV concentration, and was larger than those of nanorods or nanospheres at all CV concentrations measured. EFs were calculated as *ca* 1×10^4 and *ca* 8×10^3 for nanorods and nanospheres, respectively, at the same CV concentration (0.1 μM). It should be noted that these calculations were performed assuming that all of CV molecules in the SERS sample contributed equally to the measured SERS intensity. Certainly, it is not expected that all CV molecules added to the SERS sample adsorb with the same efficiency on the Au NPs surfaces and/or contribute to the measured signal. It is more likely that only a small fraction of molecules will contribute to the observed intensities.[3,34] Therefore, these calculated values only show a *lower limit* for the EF. The actual EFs are expected to be significantly higher.

The EF of CV on nanostars was also examined through comparison of the EF estimated using the surface area of nanospheres and surface coverage of CV, as performed in the 2-MPy case. The EF estimation was carried out with the same vibrational mode at 1618 cm^{-1}. The calculations were performed for two different reported surface areas of CV molecules, 0.4 and 4 nm^2, representing perpendicular and parallel orientations of the adsorbed molecule at the NP surface, respectively.[33] The CV concentrations needed to fully cover surface area of 150 nm gold nanospheres (with 7×10^{-13} M concentration) are calculated to be *ca* 5×10^{-7} and 5×10^{-8} M when surface areas of 0.4 and 4 nm^2, respectively, is used. Thus, the estimated EFs are *ca* 4×10^3 and *ca* 4×10^4 for perpendicular and parallel orientations, respectively. Since the surface area and concentration of nanostars could not be calculated with sufficient accuracy, the EF was also estimated by comparing the measured SERS signal with that of nanospheres. Experimentally, for both nanostars and nanorods the SERS intensity of the mode at 1618 cm^{-1} are largest when 1.6×10^{-6} M CV was used in the SERS sample. At that CV concentration, the EF of 1×10^5 and 1×10^6 for nanostars was calculated for the both perpendicular

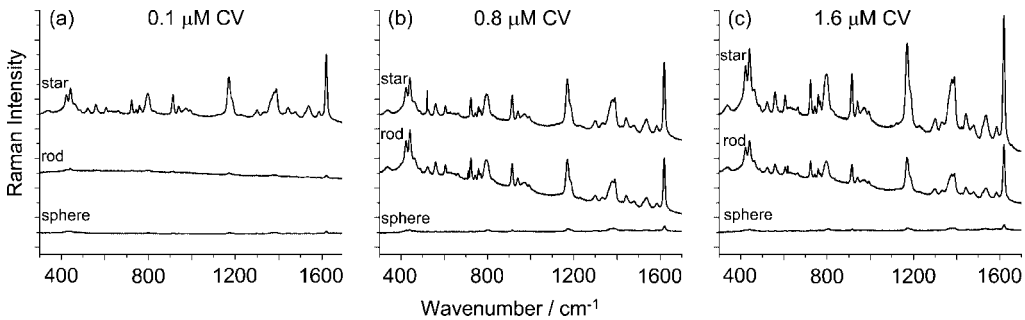

Figure 7. Comparison of SERS activity of Au NPs: nanostars (*ca* 140 nm) (top trace), nanorods (*ca* 65 nm × 30 nm (length × width)) (middle trace), and nanospheres (*ca* 150 nm) (bottom trace) for (a) 0.1 μM, (b) 0.8 μM, and (c) 1.6 μM CV used in SERS samples. The intensity scale of all three images is equivalent and the traces are offset for clarity.

This article is a US Government work and is in the public domain in the USA. Published in 2008 by John Wiley & Sons, Ltd.

and parallel orientations, respectively. Also, a similar comparison results in 5×10^4 and 5×10^5 EF for nanorods at the same CV concentration. These estimated values are obtained by assuming CV molecules to be tightly packed and that all molecules adsorbed contribute equally. If only 0.01% of the molecules in the sample contribute to the SERS intensity as reported by Kneipp *et al*.[34] the EF increases by 4 orders of magnitude and approaches 10 orders of magnitude for nanostars.

Conclusions

We observed strong and reproducible enhancement of the Raman signal from 2-MPy and CV molecules in colloidal Au nanostar solutions. Both SERS mechanisms, chemical and electromagnetic, were examined in this study. Two different molecules, 2-MPy and CV, tested on identical substrates showed dissimilar SERS activities. Also, Au colloids of similar size but different NP shapes displayed significantly disparate SERS activities. Anisotropic, 3D nanostars produced much stronger enhanced Raman modes than nanospheres for both probe molecules. Although the Raman enhancement by nanostars and nanorods was similar for 2-MPy at all studied concentrations of the molecule, it was significantly higher for nanostars compared to nanorods for CV, in particular at low concentrations of the analyte. The broad absorption band of colloidal nanostars that extends from the visible to near-IR region may be applicable to multiple laser excitations and is under investigation. Nanostars are promising additions to the family of SERS substrates.

Supporting information

Supporting information may be found in the online version of this article.

References

[1] S. E. J. Bell, N. M. S. Sirimuthu, *J. Am. Chem. Soc.* **2006**, *128*, 15580.
[2] K. Kneipp, H. Kneipp, I. Itzkan, R. R. Dasari, M. S. Feld, *Chem. Rev.* **1999**, *99*, 2957.
[3] S. M. Nie, S. R. Emory, *Science* **1997**, *275*, 1102.
[4] M. Sackmann, A. Materny, *J. Raman Spectrosc.* **2006**, *37*, 305.
[5] J. A. Baldwin, V. Blanka, M. P. Andrews, I. S. Butler, *Langmuir* **1997**, *13*, 3744.
[6] K. Kwon, K. Y. Lee, Y. W. Lee, M. Kim, J. Heo, S. J. Ahn, S. W. Han, *J. Phys. Chem. C* **2007**, *111*, 1161.
[7] J. M. Mc Lellan, Z. Y. Li, A. R. Siekkinen, Y. Xia, *Nano Lett.* **2007**, *7*, 1013.
[8] B. Nikoobakht, M. El-Sayed, *J. Phys. Chem. A* **2003**, *107*, 3372.
[9] B. Nikoobakht, J. Wang, M. El-Sayed, *Chem. Phys. Lett.* **2002**, *366*, 17.
[10] C. J. Orendorff, L. Gearheart, N. R. Jana, C. J. Murphy, *Phys. Chem. Chem. Phys.* **2006**, *8*, 165.
[11] G. C. Schatz, *Acc. Chem. Res.* **1984**, *17*, 370.
[12] V. S. Tiwari, T. Oleg, G. K. Darbha, W. Hardy, J. P. Singh, P. C. Ray, *Chem. Phys. Lett.* **2007**, *446*, 77.
[13] X. Zou, S. Dong, *J. Phys. Chem. B* **2006**, *110*, 21545.
[14] A. Tao, F. Kim, C. Hess, J. Goldberger, R. He, Y. Sun, P. Yang, *Nano Lett.* **2003**, *3*, 1229.
[15] M. Moskovits, *J. Chem. Phys.* **1978**, *69*, 4159.
[16] M. Moskovits, *Rev. Mod. Phys.* **1985**, *57*, 783.
[17] J. Jiang, K. Bosnick, M. Maillard, L. Brus, *J. Phys. Chem. B* **2003**, *107*, 9964.
[18] P. S. Kumar, I. Pastoriza-Santoz, B. Rodriguez-Gonzalez, F. Javier Garcia de Abajo, L. M. Liz-Marzan, *Nanotechnology* **2008**, *19*, 1.
[19] C. L. Nehl, H. Liao, J. H. Hafner, *Nano Lett.* **2006**, *6*, 683.
[20] D. Cialla, H. Uwe, H. Schneidewind, R. Moller, J. Popp, *ChemPhysChem* **2008**, *9*, 758.
[21] T. K. Sau, C. J. Murphy, *Langmuir* **2004**, *20*, 6414.
[22] M. Takahashi, M. Fujita, M. Ito, *Surf. Sci.* **1985**, *158*, 307.
[23] S. Eustis, M. El-Sayed, *Chem. Soc. Rev.* **2006**, *35*, 209.
[24] A. Otto, I. Mrozek, H. Grabhorn, W. Akemann, *J. Phys.: Condens. Matter* **1992**, *4*, 1143.
[25] S. L. Cumberland, G. F. Strouse, *Langmuir* **2002**, *18*, 269.
[26] D. Li, Y. Huang, L. Jinghong, *J. Colloid Interface Sci.* **2005**, *283*, 440.
[27] P. Hildebrandt, M. Stockburger, *J. Phys. Chem.* **1984**, *88*, 5935.
[28] E. J. Liang, X. L. Ye, W. Kiefer, *J. Phys. Chem. A* **1997**, *101*, 7330.
[29] L. Rivas, S. Sanchez-Cortes, J. V. Garcia-Ramos, G. Morcillo, *Langmuir* **2000**, *16*, 9722.
[30] T. Sawaguchi, F. Mizutani, S. Yoshimoto, I. Taniguchi, *Electrochim. Acta* **2000**, *45*, 2861.
[31] W. Song, Y. Wang, B. Zhao, *J. Phys. Chem. C* **2007**, *111*, 12786.
[32] I. Persaud, W. E. L. Grossman, *J. Raman Spectrosc.* **1993**, *24*, 107.
[33] A. Kudelski, *Chem. Phys. Lett.* **2005**, *414*, 271.
[34] K. Kneipp, Y. Wang, H. Kneipp, I. Itzkan, R. R. Dasari, M. S. Feld, *Phys. Rev. Lett.* **1996**, *76*, 2444.

This article is a US Government work and is in the public domain in the USA. Published in 2008 by John Wiley & Sons, Ltd.